Stereo Imaging Velocimetry for Microgravity Applications

Brian B. Miller
275 Ruth Avenue
Mansfield, OH 44907 USA

MaryJo B. Meyer and Mark D. Bethea
Mail Stop 105-1
NASA Lewis Research Center
Cleveland, OH 44135 USA

ABSTRACT

Stereo imaging velocimetry is the quantitative measurement of three-dimensional flow fields using two sensors recording data from different vantage points. The system described in this paper, under development at NASA Lewis Research Center in Cleveland, Ohio, USA, uses two CCD cameras placed perpendicular to one another, laser disk recorders, an image processing substation and a 586-based computer to record data at standard NTSC video rates (30 Hertz) and reduce it offline. The flow itself is marked with seed particles, hence the fluid must be transparent. The velocimeter tracks the motion of the particles, and from these we deduce a multi-point (500 or more), quantitative map of the flow.

Conceptually, the software portion of the velocimeter can be divided into distinct modules. These modules are: camera calibration, particle finding (image segmentation) and centroid location, particle overlap decomposition, particle tracking, and stereo matching. We will discuss our approach to each module in this paper, and give our currently achieved speed and accuracy for each where available.

1. PREVIOUS WORK

Stereo imaging velocimetry has appeared in the literature for at least twenty years, with the bulk of the research focused in Japan and the U.S. Elkins et al. reported an early stereo imaging system in 1973 which used cinematographic equipment coupled with an electronic digitizer to track several hundred particles in a turbulent flow.[1] Brodkey's group published a number of papers during the 1980's, reporting work on a multi-colored approach which allowed higher seeding densities since particles could be separated into groups according to color. This system, designed to study turbulent flow, required fine detail, so they also recorded data cinematographically, then digitized it on a high resolution field.[2] Brodkey's work was in many ways a landmark, laying the foundations for several systems developed by other researchers in later years.[3,4]

With an eye on improved understanding of internal combustion, Adamcyzk and Rimai of Ford Motor Company developed a stereo imaging system based completely on digital technology.[5] Meanwhile, two research groups in Japan independently developed their own solutions to the stereo imaging velocimetry problem.[6,7] Their work differs philosophically from the American work in that they allowed for more freedom in camera placement at the expense of a more complicated and potentially less accurate camera calibration routine. In Canada, Racca and Dewey proposed yet another approach to the SIV problem. Their work is notable, among other things, in that they chose to perform stereo matching on particles, then track these three-dimensional locations in time to reproduce particle motion.[8] Most researchers do the opposite, first tracking in two dimensions, then stereo matching the tracks to obtain the the third dimension. Lately, Guezzenec et al. have developed a commercially viable instrument.[4]

Our particular interest in stereo imaging velocimetry is focused on its potential for use in microgravity experiments performed aboard the space shuttle. These experiments are characterized by slower flows

(since convection driven by density differences is greatly lessened), model systems designed to maximize scientific returns rather than to duplicate specific earth-bound processes, cramped space, and high cost. With the exception of Guezennec's work, none of the systems developed thus far are easily adaptable to situations outside the laboratory situation for which they were invented. By using Guezennec's work as a baseline and incorporating parts of it into our own approach, we have developed the prototype velocimeter described herein.

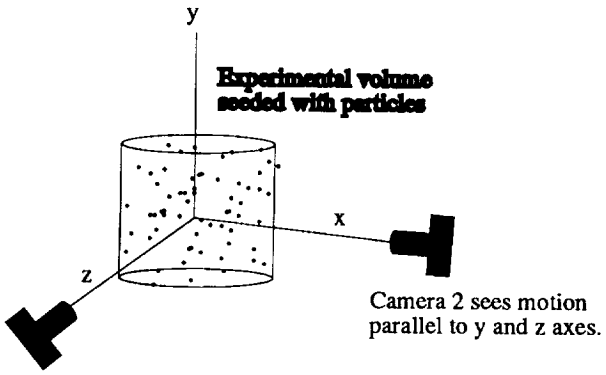

Figure 1. The two cameras are set up perpindicular to each other, so that two widely disparate views are recorded. The two views are computationally combined to obtain three dimensional coordinates of the seed particles.

2. DEFINITION AND OVERVIEW OF STEREO IMAGING VELOCIMETRY

Stereo imaging velocimetry seeks to provide a full-field, quantitative, 3-D map of any optically transparent fluid which can be seeded with tracer particles. Figure 1 shows a typical experimental set-up for our prototype. The cameras are approximately perpendicular to one another, so that one sees the x-z coordinate plane while the other sees the y-z coordinate plane. We have chosen this geometry because it maximizes the accuracy of depth perception. It also complicates the stereo matching (correspondence) problem, but we believe this shortcoming is more than compensated for by the increased accuracy in depth measurement. We define the coordinate systems of each camera to be nearly parallel to and centered on the world coordinate system, which is defined with its origin at or near the experiment's center. Small deviations, such as relative translation and rotation between the reference frames, are corrected through our camera calibration routine, which is discussed in detail below.

As the particles move with the fluid, we record two two-dimensional views of the experiment simultaneously with the cameras. These are stored in real-time on our laser disks recorders. After the experiment is completed, we read the images back off the laser disks, perform any necessary image preprocessing such as thresholding and image subtraction, and then scan the images to find the particle locations. We reduce the two dimensional images of the particles to sets of centroid coordinates which are stored in an ASCII file. Working with sets of five time steps, we determine the particle tracks as viewed by each camera, then stereo match the tracks between views to find the three dimensional locations of the particles as a function of time. Finally, we perform a consistency check on the calculated velocity field, discarding any tracks which are in significant disagreement with their neighbors.

3. INHERENT LIMITATIONS OF STEREO IMAGING VELOCIMETRY

Stereo imaging velocimetry is part of a wider field of study, all of which is aimed at producing accurate, quantitative, three-dimensional maps of arbitrarily complicated fluid flows. Other approaches include moving laser sheets, thick laser sheets (also dubbed 2 1/2 D), and holographic techniques. All of these methods, including stereo imaging velocimetry, must mark the flow in order to measure it, hence the introduction of the ubiquitous seed particles. The seed particles present a number of compromises which we recognize up front in order to meaningfully discuss the performance of our system.

The seeding density (number of seed particles per unit volume) presents one problem. Since the seed particles are effectively quantizing a continuous medium, ideally one would desire the highest possible seeding density in order to maximize spatial resolution. On the other hand, extremely high seeding

densities can themselves influence the flow, especially in solidification experiments, where they may become occluded in the solid material as it freezes. Even before this limitation is met, higher seeding densities increase the probability that foreground particles will partially or completely obscure background particles. While we have made significant software developments to minimize this effect (by deconvoluting partially overlapped particles and adding intelligence to the tracking module), it is impossible to eradicate it completely. At some point the addition of more particles to increase the data density has little or no effect on the system performance because as much data is lost as is gained. Interpolation schemes may also help alleviate the quantization effects.[9]

The choice of seed particle material is critical and varies according to the fluid system under examination. Important considerations are: wettability (we have observed one system where alumina particles in a Cesium Iodide melt migrated to the periphery and covered the ampoule walls, making it impossible to see into the experiment), chemical compatability, and a close density match between the liquid and the particles. The size of the particles is a function of the resolution of the cameras or digitization equipment, the field of view, and the particle/liquid density match. These considerations are detailed in an earlier paper.[10]

We decided to use standard NTSC signals in order to be compatible with the most hardware (cameras, storage devices, etc.) possible as well as to avoid time delays associated with chemical film develoment. A concomittant limitation is a maximum framing rate of 30 Hz. This coupled with the field of view determines the maximum velocity which the stereo imaging velocimetry system can measure. In general, if a particle moves more than 5-10% of the field of view between frames, the tracking module may fail. With an experimental volume 5 cm on a side, this amounts to a maximum velocity of 7.5-15.0 cm/sec. Another consideration is the cameras themselves. CCD cameras operate with an every-other-line scan pattern: the 1/30th second time interval between frames is divided into two 1/60 second sub-intervals. The first sub-interval is used to scan in the odd pixel lines, the second sub-interval is used to scan in the even pixel rows. This dual scan pattern can be used to double the framing rate at the expense of halving the vertical resolution: at time = 1/60 sec, the odd lines are read to find particle positions, and at time = 2/60 sec, the even lines are read to find their new positions. If the sensor field is being regarded as a whole, significant blurring effects from the CCD scan pattern occur when the particles move a pixel or more in 1/60 second. In the example above, this corresponds to a velocity of 3 mm/sec. This problem can be circumvented by using CID cameras, which do not artificially divide the sensor field. They have a true framing rate of 30 Hz.

4. CAMERA CALIBRATION

To make quantitative measurements of the motion of the tracer particles suspended in the fluid, we need an absolute coordinate system to be used as a reference to evaluate their positions. This coordinate system is the world coordinate system, and we define it such that its origin is at or near the center of the imaged experimental volume, where the principal optical axes of the two cameras have their point of nearest intersection. Each camera has its own coordinate system, which we define as tied to its image plane, with the center corresponding to the center of the pixel array, and with x and y axes extending along the rows and columns of the array and the z axis pointing along the optical axis of the lens system (see Figure 2). Since the two cameras are oriented imprecisely with respect to the world coordinate system, we need to determine the relationship between the three coordinate systems in order to correlate the two-dimensional measurements to real, three-

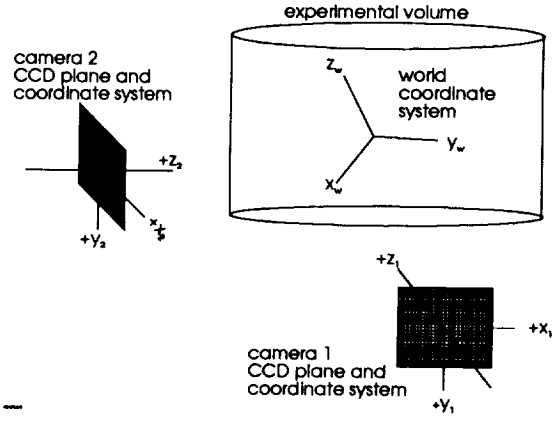

Figure 2. The relative positions of the cameras' CCD planes and coordinate systems and the world, or absolute, coordinate systems.

dimensional positions. Additionally, optical aberrations from the lenses as well as from the experiment itself, such as index of refraction mismatches, will distort the measurements if not properly taken into account. All of these corrections together are termed "camera calibration".

A variety of camera calibration methods have been developed; Weng et al.[11] give a good review of the literature. We are currently using a polynomial fitting routine.[12] The two dimensional coordinates of calibration points with known 3D locations are used to fit polynomial equations of fourth order or higher. We derive one equation for each camera. For a given camera, the equation describes a ray which crosses two computationally created calibration planes. Both of these planes are parallel to the CCD array; one is in front of the experimental volume, and the other is behind it. The polynomial equations describe the behavior of the ray between the two planes. By using a number of calibration points, we construct a number of such rays, and the best values for the fitting coefficients are determined with an averaging process. The information is organized in terms of rays in order to facilitate the stereo matching process, as explained later. For the best results, the calibration points must be distributed throughout the imaged experimental volume. We typically use at least one hundred calibration points, with resultant accuracies of better than 0.5% of full field.

5. EDGE DETECTION AND CENTROID PROCESSING

A wide variety of image analysis techniques exists for the detection of edges and the location of the centroids of particles in images. The centroid of a particle is analogous to the center of mass of a solid body. We use the centroid of a particle as a consistent means to label the location of a multi-pixel blob as a single (x, y) coordinate pair. This allows us to track a particle's motion in space. Meyer and Bethea[13] discuss the general use of this application for tracking particles in a fluid flow experiment. Wernet and Pline[14] discuss a centroid processing technique that involves applying a minimum threshold value to the image, finding the edges and processing the centroid with sub-pixel accuracy. Gonzalez and Wintz[15] describe techniques to accurately find the edges of a contour.

Our centroid algorithm accurately traces the edges of a particular multi-pixel blob and identify its centroid in order to predict the trajectory of the particle as a function of time in SIV experiments. We expect the particles in our experiments to be three to five pixels in diameter. The size is critical, because with these diameters, the particles are big enough to have a many-pixel boundary. Additionally, the particles are small enough that quantization errors around their edges can have a significant effect; the locations of their centroids can be determined accurately only by using the intensity information, which is quantized. Because the sizes of our particle images fall into this critical region, we are concerned with both an accurate edge finding routine and in preserving the intensity profiles of the particles.

Edge finding is based on using two components of the image, its gray level intensity value and its location in the 512 (i = columns) x 480 (j = rows) viewable image. It is based on the Initial Point Algorithm (IP Algorithm), which looks for the first point of a contour and the T Algorithm, which is used to trace the contour of a particle (Gonzalez and Wintz[13]). Using the Left-most-looking rule (LML), always look first at the element to the left relative to the direction that one is going. The centroid is based on using the standard center of mass equation which correlates to an intensity-weighted center of mass equation in discrete form.

$$R_{cm} = \frac{\sum_{j=j_{min}}^{j_{max}} \sum_{i=i_{min}}^{i_{max}} [i * f(i,j)\, u_x + j * f(i,j)\, u_y)]}{\sum_{j=j_{min}}^{j_{max}} \sum_{i=i_{min}}^{i_{max}} f(i,j)} \quad (1)$$

where u_x ,u_y are unit vectors, f(i,j) is the local intensity value, i and j are the column and row positions respectively, and R_{cm} is the location of the center of mass. When the edges of the particle are found, the i_{min}, i_{max}, j_{min}, and j_{max} values are stored in order to create a rectangular boundary around the particle. The algorithm uses a thresholding technique to determine a cutoff point between the background and the particles in an image. Typically, when thresholding an image, the values below the threshold are set to a specific intensity value and the values above the threshold are set to a different intensity value. This produces a binary image with two distinct intensity values, with one of the intensity values representing the object under consideration and the other representing the background. The problem with this method is that potentially useful information about the particle can be lost, and this may affect the accuracy of the centroid. For the small particles to be used in our experiments (3-5 pixels in diameter), many of the pixels will be edge pixels with intensities corresponding to a partial fill. This information is lost when using a binary thresholding routine and the location of the centroid will be less accurate unless the interior intensity information is preserved. If the threshold is selected carefully, the background will be distinct from the particles while the particles' interiors are preserved. The center of mass equation is then used to determine the center of the particle. We have tested our algorithm using synthetic, simulated, and real data. The accuracy of the algorithm is determined by the relative error between a known shape and center compared with the shape and center calculated by the algorithm. The results for all experiments were within .031 pixels (horizontal - x) and .093 pixels (vertical - y). This is assuming that all the particles are perfectly eight-connected. If the particles are not perfectly eight-connected, then a modification of the algorithm is done and combined with an overlap decomposition technique to determine the centroids for overlapping particles. Tests have shown that we can reduce up to 600 particles to centroid coordinates in less than three seconds.

6. PARTICLE OVERLAP DECOMPOSITION

The perpendicular orientation of the cameras in our SIV prototype induces a situation where the depth perception is optimal and stereo matching is the most difficult. In our system, stereo matching, is performed on particle tracks recognized in both camera views as corresponding to the same 3-dimensional location. Particle tracking is performed on five successive image frames of the fluid motion. Stereo matching is performed only with complete tracks to minimize the inherent ambiguity in the process. Thus, to maximize the data return (yield), it is necessary to obtain the maximum number of complete tracks. High yield stereo matching is impossible with high seeding densities because particles in the front of the volume obscure ones which are further away. Additionally, these overlapping particles have been shown to induce errors on the centroid location by as much as the particle radius,[16] which increases the overall error of the velocity vectors. This is called the overlapping particle problem.

A template matching approach to particle overlap decomposition has been conceived and successfully implemented[17] by other researchers. A single, average sized particle template is run over the image and any correlation peaks represent the positions of particles. Equation 2 is a mathematical description of the correlation sum used for digital representations[18]. *c(i,j)* is the result at position *(i,j)* and the template is of size *N x N*.

$$c(i,j) = \sum_{k=-N/2}^{N/2} \sum_{l=-N/2}^{N/2} x(k,l)\, y(i+k, j+l) \qquad (2)$$

For every position in the output correlation table there are $N \times N$ multiplies and $N \times N$ additions and, for an $M \times M$ table, there would be a total of $2*N^2*M^2$ computations. This represents a great deal of computational overhead for high seeding densities. Additionally, the benefits of this method are limited due to inherent variations of particle sizes and the imaging process. We have developed an alternative approach which uses multiple features to recognize overlapping particles and which has proven to be more tolerant of imaged particle size variations as well as being less computationally intensive.

Our study of SIV images determined that overlapping particles could be resolved by the human eye using four primary features: major axis length of the bounding ellipse, minor axis of the bounding ellipse, circumference, and the indentions at the point of overlap. Early algorithm development revealed that the indentions at the point of overlap could not be consistently measured due to the digitization of the CCD array, and they were not used for overlap recognition. Additionally, the minor axis length provided no information which could not be obtained from the combination of the major axis length and the circumference. Thus, our system uses only the major axis length and the circumference to recognize overlapping particles. Each particle-blob region must first be located and its centroid extracted, as described above, before particle overlap decomposition can be performed.

In general, the larger the circumference and major axis length the higher the probability that the blob region is composed of multiple overlapping particles. This provides the basis for our overlapping particle algorithm. We have used many synthetic and real images to obtain the data required for our empirically derived equations which describe these functional relationships. At reasonable seed densities in a constant volume, it is statistically improbable that a blob region will be composed of more than three overlapping particles. Thus, the probability relationships between the major axis length and the circumference were determined for up to three overlapping particles. Additionally, both the major axis of the bounding ellipse and the circumference vary linearly with respect to the particle radius. This fact is significant because the probability relationships can be "learned" for one size of particle and be transposed to other experiments through functional normalization. That is, the probability relationships are actually learned for the major axis and circumference normalized by the particle radius.

Once a blob region is located, the two recognition features can be extracted using simple image processing algorithms. The circumference is the sum of all of the "1" pixels on an 8-connected boundary, assuming the image has been appropriately thresholded.[15] The major axis length requires an elliptical approximation of the blob region. We accomplish this using the bounding ellipse algorithm presented in Haralick and Shapiro.[18] Although not presented here, the implementation of this algorithm to digital images is straight-forward because only the extremal points (left-most, top-most, bottom-most, right-most) are used in the computations. In addition to obtaining the major axis length, by-products of the algorithm are the minor axis length and the orientation of the major axis with respect to the column axis of the CCD array. These data are essential to the decomposition of the blob region into constituent centroid locations.

The probability that a blob region is a single, double, and triple particle region can be obtained following the extraction of the feature vector, (major axis length, circumference). This is accomplished by entering the features into the empirically derived probability equations described below. In all equations, x is the value of the appropriate feature.

$$P(\text{sin}\,gle) = 1 - \frac{1}{1 - e^{-\frac{x+q}{t}}}$$
$$P(triple) = 1 - \frac{1}{1 - e^{-\frac{x+b}{c}}} \qquad (3)$$
$$P(double) = 1 - P(\text{sin}\,gle) - P(triple)$$

Parameters q, t, b, and c are shown below for the major axis length and circumference, as defined by the test images described below.

Circumference

q=-8.5	t=-0.16*q
b=-16.5	c=-t

Major Axis

q=-4.0	t=-0.14*q
b=-7.3	c=-t

These values were determined for 168 micron particles at a distance of 27.5 cm from lens system to the middle of the imaged volume. Thus, the probability curves can be determined for any experimental setup by normalizing these functions with respect to these values. c and t, as a function of other parameters, remain the same and q and b are defined as:

$$q = q * \frac{\text{Particle size}}{168 \text{ microns}} * \frac{27.5 \text{ cm}}{\text{Camera Distance}}$$
$$b = b * \frac{\text{Particle size}}{168 \text{ microns}} * \frac{27.5 \text{ cm}}{\text{Camera Distance}}$$

If desired, additional normalization factors can be added to account for variations in camera parameters and lighting.

Once obtained, the maximum of the three probabilities can be used to determine the number of overlapping particles contained in the blob region. The region can be decomposed into constituent centroid locations utilizing the centroid of the blob, major axis length, minor axis length, the number of overlapping particles, and some simple geometric relationships not described here. Results from decomposing thousands of particle blob regions, at various particle sizes, lighting conditions, camera distances, etc. show that 100% of single particle regions, 83% of double particle regions, and 87% of triple particle regions are successfully decomposed using this technique. This represents a significant improvement over any existing, published technique. It should be noted that in addition to the decomposition of overlapping particles, the probabilities for all blob regions are obtained. This information provides the basis for one aspect of our prototype particle tracking technique.

7. PARTICLE TRACKING

Particle tracking is the phase of SIV where particles are identified in "N" consecutive frames and labeled as belonging to each other. Between frames, a particle is said to move in a manner consistent with the physics of fluid motion. Thus, a track is usually determined from the optimization of a penalty function which is based on the smooth variations of particle locations over small time intervals. Optimization of a penalty function can be performed using a number of different techniques. Generally speaking, traditional tracking algorithms work in the following manner: A particle is identified in frame one of the track sequence. Candidate particles are identified in frame two by searching in a sphere based on the maximum particle velocity measured in pixels. Candidate particles in frame three are identified using a position estimation for each of the possible tracks obtained from frames one and two. This process is repeated over all frames in the track sequence. Particles can be assigned to tracks on a frame by frame basis or using all possible frames in the sequence. Various researchers have utilized frame by frame optimization where a track trajectory is extended at every interval beyond the third frame.[3,8] Others have implemented a more pseudo-global technique by assigning particles to tracks only after minimizing the penalty function for all frames in the series using an exhaustive search.[4] We are currently testing two techniques. One is the exhaustive search method. The other, which we call our "prototype tracking algorithm," cannot be assigned to either of the classes described above.

7.1. Exhaustive Search Method

The exhaustive search particle tracking routine which we are currently using is self starting. This is valuable not only at the initiation of a data run, but at any given frame when particles are disappearing and reappearing from behind visual obstructions, or if the flow extends beyond the camera's field of view, so that particles are continually moving across the image boundaries. Only one piece of information need be estimated *a priori*: the maximum velocity. Converted into image frame units, the maximum velocity then sets a limit on the allowed displacement between time frames. For example, if a maximum fluid velocity translates to 300 pixels/sec or 10 pixels/frame, then the tracking algorithm will search in a 10 pixel radius in the time=t_1 frame around the time=t_0 positions of each particle. Every t_1 particle that falls within the circle is considered a potential track for the t_0 particle. A total of five time frames are searched in this manner. All the while, the software is constructing a "possible match tree", with a penalty function associated with each branch. This penalty function is compiled by noting how well the particle positions in each stage of the track follow the path projected using the velocity and acceleration information implicit in the previous frames. Once a set of five frame tracks has been established, the t_1 time frame becomes the t_0 frame, and the process begins anew. Experiments with simulated data show a five frame track to be optimal. Less than five frames results in too many wrong tracks, and more than five frames increases the processing time without significant improvements in performance.

7.2. Prototype tracking algorithm

We will describe our prototype tracker and the motivation behind it very briefly here, and in more detail in a future publication. Before attempting the development of an efficient automatic particle tracking methodology, we identified certain characteristics which we deemed necessities of the algorithm. The algorithm must be efficient, overcoming the combinatorial nature of an exhaustive search. A purely global technique was desired which not only considers all possible track combinations, but also considers the effects of all the other tracks which are competing for a particle's assignment. The tracking algorithm must minimize the effects of overlapping tracks. Finally, and most important, we wish to maximize the number of completed tracks. Our prototype tracking algorithm is striving, with a fair degree of success, to meet these goals. It utilizes a computational network to determine globally optimum tracks. Data extracted from two-dimensional particle images are mapped onto a highly interconnected network of processing elements. The data, network constraints, and flow dynamics provides the information required to track seed particles. The combinatorial complexity of particle tracking is avoided by equations of motion which efficiently guide the network to a stable solution. Overlapping tracks are overcome by

mapping the results of the probability based overlap decomposition algorithm onto the network. The algorithm is self-starting and self-terminating.

8. STEREO MATCHING

Stereo matching refers to the process of combining the two-dimensional information from the two cameras to generate three-dimensional data. With only one camera, we are able to find only the two-dimensional (x,y) location of a particle on the CCD plane. The (x,y) location of the particle in the experiment depends upon its z, or depth, coordinate. Hence with one camera, we are able to say only that the particle lies somewhere on a line which passes through its (x,y) coordinates on the CCD plane and roughly through the focal point of the camera. We construct these optical rays computationally using the two dimensional coordinates of each particle imaged on the CCD arrays along with the camera calibration information, a process akin to optical ray tracing. Stereo matching corresponds to finding the nearest intersections of the optical rays from each camera. Figure 3 illustrates how the information is used to stereo match tracks between the cameras.

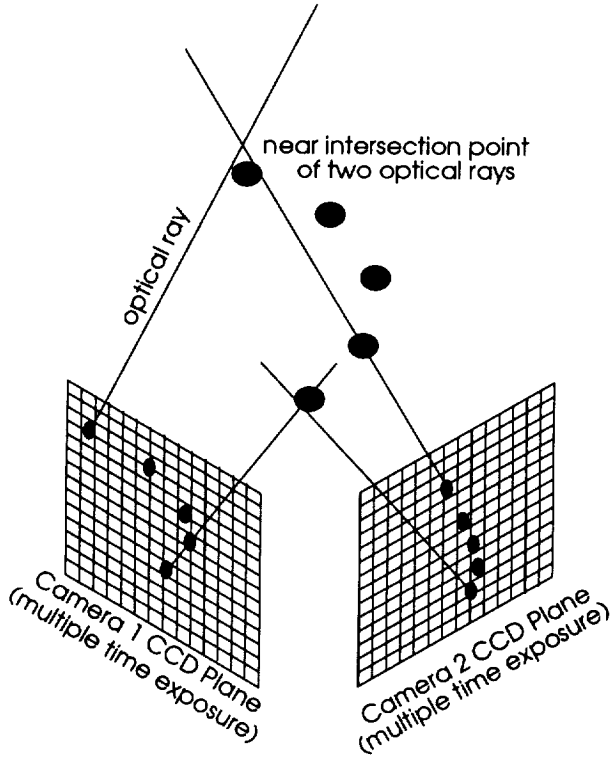

Figure 3. Stereo matching is finding the near intersections of the optical rays which cross each camera's CCD array and extend thoughout the interrogation volume. This figure illustrates the concept by showing the movement of one particle during five time slices.

We do not know in advance which track from one camera corresponds to a given track in the other. We begin by arbitrarily picking a track from one camera, then attempt stereo matching with every track imaged by the other camera. The matching is performed between each particle location in the two five frame tracks. At each location the three dimensional distance between the two candidate rays is incorporated into a penalty function. The farther the rays are from intersecting, the larger the penalty function. The penalty function is accumulated over an entire five-frame track. After comparing penalty functions for matches between one track in the left camera with every track in the right camera, we choose the match with the lowest penalty as the correct match. At this point, the three-dimensional coordinates are calculated as the locations of the nearest intersection of the optical rays. (While theoretically the lines should intersect, this almost never occurs due to the finite precision with which particles can be located in two dimensions.) We calculate the 3-D coordinates for each of the five time steps in the matched track to obtain three-dimensional, quantitative, time dependent information about the flow.

9. VELOCITY VECTOR VALIDATION

Our final check on the flow data is a velocity validation routine. This routine checks to see if any velocity vectors are outvoted by the flow field measured in its immediate vicinity. For example, a track which is perpendicular to the flow all around it would be discarded as a mistake. To perform this step, we use an adaptive Gaussian window filter to smooth the three dimensional velocity field. Each velocity vector is

then compared to the smoothed field, and if the discrepancy is greater than some prescribed limit, the vector is rejected. Typically 0.5 to 1.0% of the vectors are rejected by this procedure.

10. ACKNOWLEDGEMENTS

The work described herein has been supported through by Code UGT of the National Aeronautics and Space Administration, Washington, D.C., U.S.A.

---

11. REFERENCES

[1] R. E. Elkins, G. R. Jackman, R. R. Johnson, E. R. Lindgren and J. K. Yoo, "Evaluation of Stereoscopic Trace Particle Records of Turbulent Flow Fields," Review of Scientific Instruments, Vol. 48, No. 7, pp. 738-746, 1977.

[2] R. S. Brodkey, "Image Processing and Analysis for Turbulence Research," Chemical Engineering Education, Fall 1986, pp. 203-207.

[3] T. P. Chang, N. A. Wilcox, and G. B. Tatterson, "Application of Image Processing to the Analysis of Three-Dimensional Flow Fields," Optical Engineering, Vol. 23, No. 3, pp. 283-287, 1984.

[4] Y. G. Guezennec, R. S. Brodkey, N. Trigui, and J. C. Kent, "Algorithm for Fully Automated Three Dimensional Tracking Velocimetry," accepted for publication in Experiments in Fluids.

[5] A. A. Adamczyk and L. Rimai "Reconstruction of a 3-Dimensional Flow Field From Orthogonal Views of Seed Track Video Images," Experiments in fluid, Vol. 6, pp. 380-386, 1988.

[6] K. Nishino, N. Kasagi, and M. Hirata, "Three-Dimensional Particle Tracking Velocimetry Based on Automated Digital Image Processing," Trans. of the ASME, Vol. 111, pp. 384-391.

[7] T. Kobayashi, T. Saga, and K. Sekimoto, "Velocity Measurement of Three-Dimensional Flow Around Rotating Parallel Disks by Digital Image Processing," ASME Winter Annual Meeting, San Francisco, 1989.

[8] R. G. Racca and J. M Dewey, "A Method for Automatic Particle Tracking in a Three-Dimensional Flow Field," Experiments in Fluids, Vol. 6, pp. 25-32, 1988.

[9] N. L. Mangla and S. K. Sinha, "Application of Computer-Aided Optimization in Particle Tracking Velocimetry," IMACS International Symposium on Mathematical Modelling and Scientific Computing, Bangladore, India, December 7-11, 1992.

[10] M. B. Meyer, M. D. Bethea, Y. G. Guezennec, and W. C. Choi, "Stereo Imaging Velocimetry: A New Option for Microgravity Experiments," ASME Winter Annual Meeting, New Orleans, 1993, AMD-Vol. 174/FED-Vol. 175, Fluid Mechanics Phenomena in Microgravity, pp. 173-182.

[11] J. Weng, P. Cohen and M. Herniou, "Camera Calibration with Distortion Models and Accuracy Evaluation," IEEE Transactions of Pattern Analysis and Machine Intelligence, Vol. 14, No. 10, pp. 965-980, 1992.

[12] J. C. Kent, N. Trigui, W. C. Choi, Y. G. Guezennec, and R. S. Brodkey, "Calibrated Photogrammetric Transform for Three Dimensional Particle Tracking Velocimeter", Proceeding of SPIE Congerence on Optical Diagnostics in Fluid and Thermal Flow, San Diego, 1993.

[13] M. B. Meyer and M. D. Bethea, "A Full Field, 3-D Velocimeter for NASA's Microgravity Science Program, AIAA 30th Aerospace Sciences Meeting and Exhibit, AIAA-92-0784, 1992.

[14] M. P. Wernet and A. D. Pline, "Particle Image Velocimetry for Surface Tension Driven Convection Experiment Using a Particle Displacement Tracking Technique", Proceedings from ASME Topical Meeting on Laser Anemometry, Cleveland, OH, 1991, Vol. 1, 315-325.

[15] R. C. Gonzalez and P. Wintz, "Digital Image Processing, First Edition," Addison-Wesley, Reading, Massachusetts, 1977, pp. 253-261.

[16] Y. G. Guezennec and N. Kiritsis, "Statistical Investigaton of Errors in Particle Imaging Velocimetry," Experiments in Fluids, Vol. 10, pp. 138-146.

[17] N. Trigui, Y. G. Guezennec, R. Brodkey, and C. Kent, "Fully Automated Three-Dimensional Particle Image Velocimetry System Applied to Engine Fluid Mechanics Research," Proceedings of Optical Methods and Data Processing in Heat and Fluid Flow, London, April, 1992.

[18] R. M. Haralick and L. G. Shapiro, "Computer and Robot Vision, Vol. 1", Addison-Wesley, Reading, Massachusetts, 1992.